

^1H NMR study of hydrogen in quasicrystalline $\text{Ti}_{0.45-x}\text{V}_x\text{Zr}_{0.38}\text{Ni}_{0.17}$

A. Shastri*

Ames Laboratory, U.S.D.O.E. and Department of Physics and Astronomy, Iowa State University, Ames, Iowa 50011

E. H. Majzoub

*Department of Physics, Washington University, Campus Box 1105, One Brookings Dr., St. Louis, Missouri 63130-4899*F. Borsa[†]*Ames Laboratory, U.S.D.O.E. and Department of Physics and Astronomy, Iowa State University, Ames, Iowa 50011*

P. C. Gibbons and K. F. Kelton

Department of Physics, Washington University, Campus Box 1105, One Brookings Dr., St. Louis, Missouri 63130-4899

(Received 29 September 1997)

^1H nuclear-magnetic-resonance (NMR) spectra and spin-lattice relaxation rates (R_1) were studied in the hydrogenated $\text{Ti}_{0.45-x}\text{V}_x\text{Zr}_{0.38}\text{Ni}_{0.17}$ quasicrystal for $x=0.00, 0.02$, and a hydrogen-to-metal-atom ratio (H/M) = 1.88. NMR measurements were made from 4 to 550 K at resonance frequencies of 8, 18, 55, and 200 MHz. Theoretical ^1H second-moment values (M_2) were calculated based on Bergman and Mackay cluster models and compared with experimental M_2 values. The R_1 data reveal a distribution of activation energies for the ^1H diffusion through the quasilattice; the distribution is insensitive to the vanadium concentration, x . Low-temperature R_1 data reveal an additional low-temperature relaxation mechanism that is not yet well understood. [S0163-1829(98)02409-6]

I. INTRODUCTION

It has been demonstrated that quasicrystals (QC's), materials that simultaneously possess forbidden crystallographic symmetry and long-range translational order,¹ can, under appropriate conditions, absorb large amounts of hydrogen.² As with many hydrogen-loaded crystalline and amorphous materials,³ there is great interest in potential technological applications,⁴ and hydrides have been studied using a wide variety of experimental techniques.⁵ In particular, the application of nuclear magnetic resonance (NMR) in hydrogen-loaded systems to obtain information about local environments of metal and hydrogen sites, as well as hydrogen kinetics, is well known.^{3,6-8} NMR investigations of hydrogen in quasicrystals have the potential to (1) test current structural models of local order and therefore shed light on local quasicrystalline order; and (2) to provide both a quantitative and qualitative understanding of hydrogen motion within the quasilattice, which may be useful for further improving hydrogen storage properties.

There have been many NMR investigations of the metal-atom nuclei in QC systems.⁹ With the loading of hydrogen into titanium-based quasicrystals,² and the development of cluster models that describe the location of hydrogen interstitial sites,¹⁰ the possibility of checking the consistency of ^1H NMR data with local models of quasicrystalline order has emerged. Few studies currently exist of proton NMR in quasicrystalline systems.¹¹ In particular, the icosahedral (i) phase $\text{Ti}_{0.45}\text{Zr}_{0.38}\text{Ni}_{0.17}$ quasicrystalline system has become a focal point of interest, and ^1H NMR has been studied on samples having hydrogen-to-metal-atom ratios (H/M) of 1.42.¹¹ However, these measurements were complicated by the nonuniform hydrogenation of the i phase, as well as by

the presence of hydride precipitates of hexagonal Laves phases. Improvements in hydrogen-loading techniques have resulted in phase pure, uniformly hydrogenated $\text{Ti}_{0.45-x}\text{V}_x\text{Zr}_{0.38}\text{Ni}_{0.17}$ quasicrystalline samples with a maximum hydrogen content of $\text{H}/\text{M} = 1.88$.¹²

We present here a ^1H NMR study of the hydrogen-loaded $\text{Ti}_{0.45-x}\text{V}_x\text{Zr}_{0.38}\text{Ni}_{0.17}$ i-phase system with $\text{H}/\text{M} = 1.88$. The ^1H NMR spectrum will be analyzed in the light of proposed models of the local environment.¹⁰ Measurements of the ^1H nuclear spin-lattice relaxation rate were made in order to extract information about ^1H diffusion through the quasilattice.

II. EXPERIMENTAL

The $\text{Ti}_{0.45-x}\text{V}_x\text{Zr}_{0.38}\text{Ni}_{0.17}$ quasicrystals were prepared by melt spinning, as described elsewhere.¹³ Some of the rapidly quenched ribbons were powdered and characterized by x-ray diffraction to determine their quality and phase purity. Hydrogen was loaded into the quasicrystal ribbons electrolytically by cathodically biasing the sample 3.5 volts with respect to a platinum anode in a 5 M solution of KOH. X-ray diffraction of the hydrogen-loaded i phase indicated no impurity phases were present. By weighing the samples before and after hydrogen absorption, it was determined that $\text{H}/\text{M} = 1.88$ for both $x=0.00$ and 0.02 samples. This value also agreed with that computed from shifts in the quasicrystal diffraction peaks with hydrogenation.

The NMR measurements were performed with home-built, phase-coherent, pulse Fourier transform spectrometers. Except for the proton NMR data at 200 MHz, all NMR data were collected using a Varian V-3800 electromagnet. The 200 MHz data were taken using an Oxford Instruments 4.7 T

TABLE I. Experimental values of the second moment M_2^{exp} in $\text{Ti}_{0.45-x}\text{V}_x\text{Zr}_{0.38}\text{Ni}_{0.17}\text{H}_{1.88}$ for $x=0, 0.02$ obtained by fitting a Gaussian function $f(\omega)=A \exp[-(\omega-\omega_0)^2/2M_2]$ to proton NMR spectra. The method of calculating M_2^{theory} is described in the text.

X	M_2^{exp} (s^{-2})	Bergman cluster		Mackay cluster	
		M_2^{theory} (s^{-2})	$M_2^{\text{exp}}/M_2^{\text{theory}}$	M_2^{theory} (s^{-2})	$M_2^{\text{exp}}/M_2^{\text{theory}}$
0.00	$(5.81 \pm 0.02) \times 10^{10}$	1.46×10^{10}	3.97	0.303×10^{10}	19.2
0.02	$(6.22 \pm 0.06) \times 10^{10}$	1.49×10^{10}	4.17	0.309×10^{10}	20.1

superconducting magnet. ¹H NMR spectra were obtained by taking the Fourier transform of the ¹H free induction decay following a $\pi/2$ pulse with pulse length $\tau=1\mu\text{s}$. This pulse was sufficiently short to uniformly irradiate the approximately 90 kHz full width half maximum proton NMR spectrum that was observed at temperatures for which proton diffusion was frozen out. This ‘‘rigid-lattice’’ line shape $f(\omega)$ was fit to a Gaussian function $f(\omega)=A \exp[-(\omega-\omega_0)^2/2M_2]$, and the second moment M_2 was extracted as a parameter of the fit. The quality of the fits was high, and the uncertainty in the M_2 values was less than 1%. In addition, the ¹H spin-lattice relaxation rate (R_1) was determined by measuring the decay of the normalized z component of the nuclear magnetization $m(t)$, defined as $m(t)=M_z(\infty)-M_z(t)/M_z(\infty)$. The $m(t)$ data were obtained by saturation and inversion recovery methods above and below 150 K ($1000/T=6.67\text{K}^{-1}$), respectively. The recovery was exponential over two decades, and R_1 was obtained by fitting $m(t)$ to a simple exponential function $f(t)=C \exp(-R_1t)$, where C and R_1 were parameters of the fit. For measurements from 150 to 550 K ($1000/T=1.81\text{K}^{-1}$), the powdered samples were sealed in Pyrex tubes at 10^{-2} torr of argon gas pressure to reduce possible oxidation of the sample at high temperatures. This study was done at temperatures below 600 K ($1000/T \geq 1.67\text{K}^{-1}$), the temperature at which samples begin to evolve hydrogen.¹⁴

III. RESULTS AND DISCUSSION

A. Analysis of the proton NMR spectrum

The ¹H NMR spectra were taken at 50 K ($1000/T=20\text{K}^{-1}$), a temperature well below the point at which thermally activated hopping begins to narrow the NMR line. The experimental second moments from the rigid lattice proton NMR line are given in Table I.

We now discuss the interactions that determine the proton NMR line. NMR data in hydrides may usually be understood by writing the total Hamiltonian as $H=H_Z+H_D+H_E$, where H_Z is the Zeeman term, H_D is from the nuclear dipole-dipole coupling, and H_E arises from the coupling of the nuclear spin to localized electronic magnetic moments of the host metal. However, if the term H_E were present, one expects an inhomogeneous broadening that scales as H_0/T , where H_0 is the applied magnetic field strength and T is temperature. The rigid lattice linewidth was independent of field and temperature, indicating that the transition metal ions do not carry a local moment. The field independence also excludes the possibility of the line shape being a distribution of Knight shifted lines, which would also scale pro-

portionally to H_0 . Therefore, assuming only the dipolar term contributes to the perturbation of the nuclear Zeeman levels, M_2 may be written as

$$M_2=M_2^H+M_2^{IS}, \quad (1)$$

where homonuclear term M_2^H arises from the dipole interactions of like nuclei, i.e., H-H interactions; and the heteronuclear term M_2^{IS} arises from the dipole interactions of unlike nuclei, i.e., H-X where $X=\text{Ti}, \text{V}, \text{Ni}, \text{Zr}$ ¹⁵ Because the decoration of the quasilattice with metal atoms is unknown, the term M_2^{IS} , which depends on the H-X separation distances, cannot be calculated exactly. We will therefore ignore M_2^{IS} for the moment, but will discuss estimates of its magnitude in a following paragraph. The powder averaged, homonuclear second moment is given by

$$M_2^{\text{theory}}=\frac{3}{5}\hbar^2\gamma_I^4I(I+1)\sum_i\frac{p_i}{r_{ij}^6}, \quad (2)$$

where γ_I is the proton’s gyromagnetic ratio, I is the proton spin, the summation is over all interstitial sites i occupied with probability p_i , and r_{ij} is the distance from a fixed proton site j to all the interstitial sites i .¹⁵

To perform the summation of Eq. (2), we used the Bergman and Mackay cluster models proposed by Viano.¹⁰ Both models consist of two concentric icosahedra, the radius of the outer one being twice that of the inner one. In the Bergman cluster, metal atoms reside on inner and outer vertices and on outer face centers, and in the Mackay cluster, on vertices and outer edge centers, of the nested icosahedra. Hydrogen occupy some of the distorted tetrahedral sites within the cluster, and are not allowed to simultaneously occupy neighboring sites that are closer together than 2.1 Å [Switendick criterion (Ref. 16)]. The summation of Eq. (2) was performed by picking the fixed interstitial site j to be within the inner icosahedron, and performing the summation over all allowed sites within the Bergman or Mackay cluster. The model does not include the linkages between the clusters. X-ray-diffraction studies of the $\text{Ti}_{0.45-x}\text{V}_x\text{Zr}_{0.38}\text{Ni}_{0.17}$ samples set the radii of the hydrogenated clusters at $a_i=5.56$ and 5.54 Å for the $x=0.00$ and 0.02 samples, respectively.

The M_2^{theory} values for the two models are given in Table I. We note that M_2^{theory} is smaller than M_2^{exp} in both models: the ratio $M_2^{\text{exp}}/M_2^{\text{theory}} \approx 4$ and 20 for the Bergman and Mackay clusters, respectively. The shorter average H-H distances of the Bergman cluster results, through Eq. (2), in a larger M_2^{theory} and therefore better agreement than the Mackay cluster, and it is the Bergman cluster we focus on in

the subsequent discussion. This choice of the Bergman cluster for this quasicrystal is supported by a recent structural study of the 1/1 phase, showing that it is isomorphic with the Bergman and R phases.¹⁷

This discrepancy between M_2^{theory} and M_2^{exp} cannot be explained as a result of neglecting M_2^{IS} . We estimated M_2^{IS} by assuming the metal atoms randomly populate the vertices of the cluster. For each nuclear species, one has a heteronuclear contribution

$$M_2^{\text{IS}} = \frac{4}{15} \gamma_I^2 \gamma_S^2 S(S+1) \sum_i \frac{p_i}{r_i^6}$$

(Ref. 15), where p_i is given by the atomic percent of the nuclear species in the stoichiometry of the cluster. We assumed the isotopic parameters that would maximize the sum, and added together the contributions for the Ti, V, Ni, and Zr nuclei. Combining the results of this calculation with the values in Table I, one finds a total $M_2 = M_2^{\text{II}} + M_2^{\text{IS}}$ of $2.62 \times 10^{10} \text{ s}^{-2}$ and $3.04 \times 10^{10} \text{ s}^{-2}$ for the $x=0$ and 0.02 samples, respectively. For the Bergman cluster, this results in $M_2^{\text{exp}}/M_2^{\text{theory}} = 2.22$ and 2.04 for the $x=0, 0.02$ samples, respectively, and indicates that though the estimated M_2^{IS} is not negligible, it cannot explain the differences between theoretical and experimental values. Another possibility is that the contribution to M_2^{theory} from the linkages between clusters is not negligible. Though the structure of the cluster linkages is unknown, a simple estimate shows the linkages must contain a substantial amount of hydrogen: the experimental value of $\text{H}/\text{M} = 1.88$ for our $\text{Ti}_{0.45-x}\text{V}_x\text{Zr}_{0.38}\text{Ni}_{0.17}$ samples is 1.7 times larger than the theoretical value obtained from the Bergman cluster model,¹⁰ indicating that the summation of Eq. (2) ignores a substantial fraction of hydrogen in the sample. In addition, short interstitial site distances within linkages might be another factor contributing to the discrepancy. We can increase the number of hydrogen atoms within the inner icosahedral shell of metal atoms by moving the hydrogen outward, away from the center, but not so far that they overlap the first-shell metal atoms.¹⁸ Each of the eight inner hydrogen atoms can have six first hydrogen neighbors at the Switendick distance of 2.1 Å. In this model $M_2^{\text{theory}} = 2.03 \times 10^{10} \text{ s}^{-2}$ for the Bergman cluster at $x=0.00$, larger than the value in Table I, but still not in agreement with the observed value. Finally, if one ignores the Switendick criterion and performs the summation over all interstitial sites within the Bergman cluster, one finds an upper limit on the second moment of $M_2^{\text{theory}} = 37 \times 10^{10} \text{ s}^{-2}$ that is larger than M_2^{exp} . If the Switendick criterion is violated for one pair of sites with a separation of 1.4 Å, it is possible to get agreement with experiment within 10%. Though it is unlikely that such close proton-proton separations occur physically, one should not rule out violation of the Switendick criterion to a lesser degree.

B. Analysis of relaxation data

The proton spin-lattice relaxation rates R_1 are shown in Fig. 1 for both samples. In many metal hydride systems without paramagnetic impurities, the relaxation rate may be written as

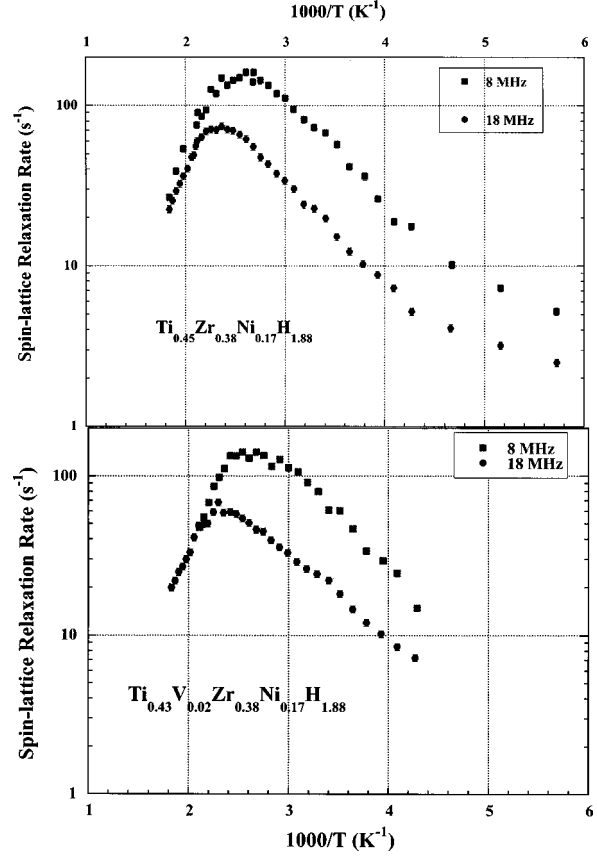


FIG. 1. ^1H nuclear spin-lattice relaxation rates R_1 vs reciprocal temperature $1000/T$ in icosahedral $\text{Ti}_{0.45-x}\text{V}_x\text{Zr}_{0.38}\text{Ni}_{0.17}\text{H}_{1.88}$ for $x = 0.00$ and 0.02 at 8 and 18 MHz.

$$R_1 = R_{1d} + R_{1e}, \quad (3)$$

where R_{1d} and R_{1e} are the contributions to the relaxation rate from dipolar and electronic contributions, respectively. In transition metal alloys, electrons at the Fermi energy (E_F) will typically occupy both s and d orbitals. As long as E_F does not fall on a sharp peak in the density of states, the Korringa model predicts $R_{1e} = AT$, where A is a constant independent of H_0 .³ Low-temperature R_1 measurements (Fig. 2), to be discussed in detail later, were interpreted within the Korringa model to yield $A = (7.0 \pm 0.5)$

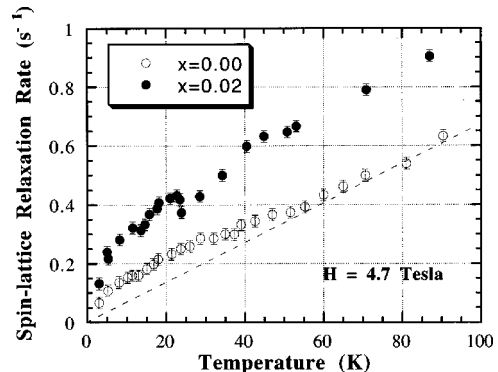


FIG. 2. ^1H nuclear spin-lattice relaxation rates R_1 vs temperature in icosahedral $\text{Ti}_{0.45-x}\text{V}_x\text{Zr}_{0.38}\text{Ni}_{0.17}\text{H}_{1.88}$ for $x = 0.00$ and 0.02 at 200 MHz. The dotted line represents the electronic contribution.

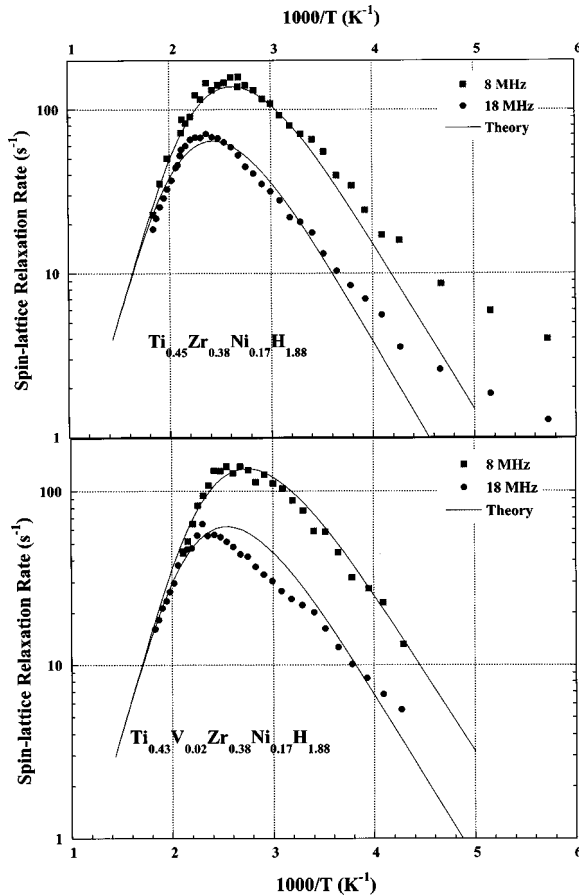


FIG. 3. ¹H nuclear spin-lattice relaxation rates for icosahedral $\text{Ti}_{0.45-x}\text{V}_x\text{Zr}_{0.38}\text{Ni}_{0.17}\text{H}_{1.88}$ after the electronic term R_{1e} has been subtracted from the R_1 values of Fig. 1. The theoretical curve is obtained using Eq. (5) as described in the text, and fit parameters are listed in Table II.

$\times 10^{-3} \text{ s}^{-1} \text{ K}^{-1}$ for the $x=0.00$ sample. The $x=0.02$ data were difficult to interpret in this model because the low-temperature data were not linear, and it was assumed initially that the electronic contribution was the same as for the $x=0.00$ sample. Subtracting off the electronic contribution from the R_1 data yielded the dipolar relaxation rate data R_{1d} of Fig. 3.

The relaxation rate due to like spins coupled by the magnetic dipole-dipole interaction and undergoing relative translation diffusion may be written¹⁵ as

$$R_{1d} = B \left(\frac{\tau_C}{1 + \omega^2 \tau_C^2} + \frac{4\tau_C}{1 + 4\omega^2 \tau_C^2} \right),$$

$$B = \frac{2M_2}{3}, \quad (4)$$

where M_2 is given by Eq. (2), and ω is the proton Larmor frequency. This formulation is based on the usual Lorentzian [so-called Bloembergen-Purcell-Pound (BPP)] spectral densities corresponding to correlation functions that decay exponentially with correlation time τ_C .¹⁹ We make the usual assumption that the correlation time follows an Arrhenius relation $\tau_C = \tau_\infty \exp(E_a/k_B T)$, where E_a is the energy barrier to thermally activated hopping and the prefactor τ_∞ is called

the dwell time. We note that lattice specific models of correlation functions exist, but have been developed only for simple crystalline structures. In addition, although the BPP model can yield τ_C values that differ by a factor of two or more, the E_a values have usually been reliable to within 10% in crystalline and amorphous systems when direct comparisons were possible with values obtained by other techniques.³ For these reasons, we will apply the BPP model to our analysis of quasicrystals.

When all diffusion pathways are characterized by a single activation energy, the above theory predicts $R_{1d} \propto \tau_C$ when $\omega\tau_C \ll 1$ (high T limit) and $R_{1d} \propto (\omega\tau_C)^{-1}$ when $\omega\tau_C \gg 1$ (low T limit). The theoretical maximum relaxation rate has a magnitude of $R_{1d}^{\text{max}} = 0.95M_2/\omega$ and occurs when $\omega\tau_C = 0.615$. Semilog plots of R_1 vs $1/T$ data would be expected to have constant slopes proportional to $\pm E$ in the low- and high-temperature limits and the curves would therefore appear symmetric about the maximum in the BPP curve. The data of Fig. 3 are not symmetric and the experimental value of R_{1d}^{max} is almost a factor of 7 smaller than the theoretical value. Reports of similar differences between Eq. (4) and experimental data exist in crystalline and noncrystalline systems.²¹⁻²³

The asymmetry of the relaxation curve suggests a distribution of diffusion pathways each with its own activation energy.²³ The relaxation rate may be calculated by integrating Eq. (4) over the distribution $g(E)$ (Refs. 20, 21, and 23)

$$R_1^{\text{theory}} = B \int_0^{+\infty} dE g(E) R_{1d}(E). \quad (5)$$

We assumed a Gaussian distribution of activation energies $g(E) = 1/\sigma\sqrt{2\pi} \exp[-(E-E_a)^2/2\sigma^2]$, calculated the R_1^{theory} for data at 8 and 18 MHz by adjusting the free parameters E_a , τ_∞ , σ , B , and required that the parameters describe data at both frequencies. The parameter E_a was adjusted to make the theoretical curve parallel to the experimental curve at low and high temperatures. The parameter τ_∞ was then modified to make the BPP maximum of the theoretical curve approximately the same as the experimental data. Finally, σ and B were altered to achieve the final fit, the results of which are shown in Fig. 3. The fit parameters are listed in Table II and result in correlation times of $\tau_C = (1.7 \times 10^{-13} \text{ s}) \exp(E/k_B T)$ where $E = 0.35$ and 0.33 eV for $x = 0.00$ and 0.02 , respectively.

We now discuss the physical significance of the values of the parameters in the model. The most important point is that the distribution can explain the asymmetry in the relaxation peaks. That the TiVNiZr quasicrystals should exhibit a distribution of activation energies is not surprising. NMR studies of metal atoms in many quasicrystalline systems reveals broad distributions of local fields⁹ at the metal atoms sites. A distribution of local fields may arise from a multitude of decorations of the icosahedral cluster by the metal atoms, thereby giving rise to a distribution of energy barriers to hydrogen diffusion through interstitial sites. In addition, (1) the mean activation energy E_a for the samples from Table II is within 1% of E_a values reported in Ref. 11 in samples with $H/M = 1$, and is similar to values found in many amorphous hydride systems.^{3,20,21} Thus the E_a values do not appear sensitive to hydrogen concentration within experimental

TABLE II. Parameters for icosahedral $\text{Ti}_{0.45-x}\text{V}_x\text{Zr}_{0.38}\text{Ni}_{0.17}\text{H}_{1.88}$ obtained by fitting the curve of Eq. (5) to the data of Fig. 3.

X	τ_∞ (s)	\bar{E} (eV)	σ (eV)	B (s^{-2})
0.00	1.7×10^{-13}	0.35	0.052	0.8×10^{10}
0.02	1.7×10^{-13}	0.33	0.052	0.8×10^{10}

uncertainty. (2) The value of the prefactor τ_∞ in Table II may be compared with a theoretical value based on a simple model. If one assumes that the protons sit in potential wells that are sinusoidal with depth E_a and separation d , the phonon driven attempt frequency (PDAF) for barrier hopping is $f = N_v \sqrt{E_a/2m}/d$ where m is the proton mass and N_v is the number of vacant nearest-neighbor interstitial sites into which the proton may hop.²³ Taking the value of E_a from Table II, the average well separation between interstitial sites to be $d = 2.5 \text{ \AA}$, and $N_v \approx 1$, one finds $f = 2.0 \times 10^{13} \text{ s}^{-1}$. The experimental value of $1/\tau_\infty = 5.8 \times 10^{12} \text{ s}^{-1}$ obtained from the τ_∞ value of Table II differs from the PDAF by only a factor of 3.4, which constitutes reasonable agreement given the simplicity of the PDAF model. We conclude that the τ_∞ value obtained is reasonable.

A word should be said about the deviation of the theoretical curve from experimental values below 300 K (above $1000/T = 3.33 \text{ K}^{-1}$) in Fig. 3. The deviation is not due to the electronic contribution to the relaxation, which was subtracted off. Nor can the deviation be explained by including the relaxation of ^1H due to the unlike spins in the alloy. The effect of the Ti atoms was included by using BPP formulas for unlike spins,¹⁵ and the contributions from like spins [Eq. (4)] and unlike spins were added and integrated over a Gaussian distribution as in Eq. (5). However, this did not explain the deviation. Still another possibility is that the underlying distribution of activation energies may not be Gaussian. Though other distributions were tried, we were not able to find a simple distribution that worked over the entire temperature range, implying that the distribution is more complicated or that the approach of Eq. (5) is oversimplified.

We return now to discuss the low-temperature R_1 data of Fig. 2. The data taken from the $x=0.00$ sample shows a linear dependence between 55 and 90 K that extrapolates to the origin. This behavior we attribute to relaxation of the protons by s - and d -band conduction electrons.³ Below 55 K, however, the relaxation rate is not linear in temperature, implying that an additional relaxation mechanism is present. A similar effect was reported in the crystalline ScH_x system,²² and therefore the effect is not specifically related to quasicrystallinity. Subtracting off the conduction electron contribution $R_{1e} = (7.0 \pm 0.5) \times 10^{-3} \text{ T s}^{-1}$ from the R_1 data of Fig. 2 gives the data of Fig. 4. The source of the additional relaxation is interesting and is a point for debate. Lichty *et al.* explained similar behavior in ScH_x using a model that included localized hopping between closely spaced interstitial sites.²² Assuming this relaxation is due to thermally activated hopping and applying Eq. (5) and the procedure discussed previously to extract fit parameters, $E_a = 4.3 \times 10^{-3} \text{ eV}$, $\sigma = 3.4 \times 10^{-3} \text{ eV}$, $\tau_\infty = 2.4 \times 10^{-11} \text{ s}$, and $B = 1.7 \times 10^8 \text{ s}^{-2}$. The fit is shown in Fig. 4. The motion is described by barriers with E_a nearly 1% the value at high temperature, but by

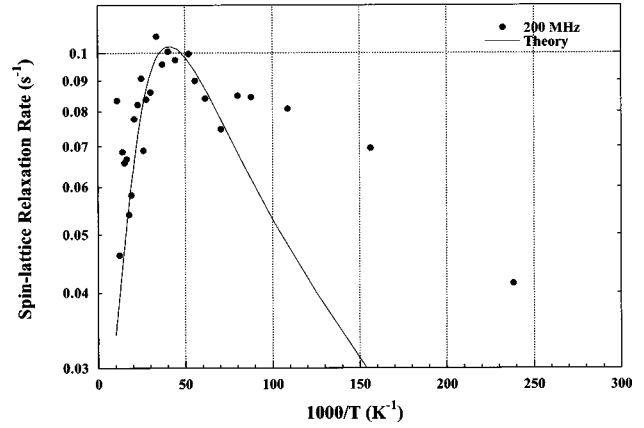


FIG. 4. ^1H nuclear spin-lattice relaxation rates for icosahedral $\text{Ti}_{0.45-x}\text{Zr}_{0.38}\text{Ni}_{0.17}\text{H}_{1.88}$ at 200 MHz after the electronic term R_{1e} has been subtracted from the data of Fig. 2. The theoretical curve is obtained using Eq. (5), and fit parameters are listed in the text.

a dwell time τ_∞ that is nearly 100 times larger than the value at high temperature. That such small energy barriers should result in such long correlation times is unsatisfying, and suggest that thermally activated hopping may not be the correct diffusion mechanism at low temperatures. Lichty *et al.* also found small E_a values in the ScH_x system. Svare and co-workers²⁴ reinterpreted the low-temperature Sc_xH data of Lichty *et al.* in terms of hydrogen tunneling between asymmetric potential wells of closely spaced interstitial sites. In Sc_xH , interstitial sites can be as close as 1.3 \AA apart, and filling a pair of sites with a proton can result in tunneling of the proton between the site potential wells. Given that the Bergman cluster model also provides proton nearest-neighbor sites of 1.3 \AA , the tunneling model is a reasonable possibility.

IV. CONCLUSIONS

In summary, we have presented an ^1H NMR study of the hydrogenated $\text{Ti}_{0.45-x}\text{V}_x\text{Zr}_{0.38}\text{Ni}_{0.17}$ i-phase system with $\text{H}/\text{M} = 1.88$ and $x = 0.00$ and $x = 0.02$. Values of M_2^{theory} favor the Bergman cluster model over the Mackay, though M_2^{theory} differs from M_2^{exp} by a factor of 4. The discrepancy is probably due to neglecting linkages between icosahedral clusters. The high-temperature hydrogen diffusion is characterized by thermally activated hopping of protons over a wide distribution of energy barriers, which arise from the local quasicrystalline order through a broad distribution of local fields. The low-temperature nuclear relaxation mechanism is not well described by thermally activated hopping, and may be due to proton tunneling between closely spaced interstitial sites.

ACKNOWLEDGMENTS

The authors gratefully acknowledge helpful suggestions from N. Adolphi and the late D. R. Torgeson, and technical assistance from R. Hennig and J. Ostenson. Ames Laboratory is operated for the U. S. Department of Energy by Iowa State University under Contract No. W-7405-Eng-82.

- *Present address: Department of Radiology, Medical University of South Carolina, 107 Ashley Avenue, Charleston, SC 29425.
- †Also at Dipartimento di Fisica, Università di Pavia, 27100 Pavia, Italy.
- ¹P. J. Steinhardt and S. Ostlund, *The Physics of Quasicrystals* (World Scientific, New Jersey, 1987); A. I. Goldman and M. Widom, *Annu. Rev. Phys. Chem.* **42**, 685 (1991).
- ²A. M. Viano, R. M. Stroud, P. C. Gibbons, A. F. McDowell, M. S. Conradi, and K. F. Kelton, *Phys. Rev. B* **51**, 12 026 (1995).
- ³R. C. Bowman, in *Hydrogen in Disordered and Amorphous Solids*, edited by G. Bambakidis and R. C. Bowman (Plenum, New York, 1986), p. 237.
- ⁴J. J. Reilly and G. D. Sandrock, *Sci. Am.* **242**, 118 (1980).
- ⁵L. Schlapbach, in *Hydrogen in Intermetallic Compounds I*, edited by L. Schlapbach (Springer-Verlag, New York, 1988).
- ⁶R. M. Cotts, *Hydrogen in Metals I: A Basic Properties*, edited by G. Alefeld and J. Voelkl (Springer-Verlag, New York, 1978), p. 227.
- ⁷R. G. Barnes, in *Nuclear and Electron Spectroscopies Applied to Material Sciences*, edited by E. N. Kaufman and G. Shenoy (Elsevier, Amsterdam, 1981), p. 19.
- ⁸D. R. Torgeson, in *Encyclopedia of Nuclear Magnetic Resonance*, edited by D. M. Grant and R. K. Harris (Wiley, New York, 1996), Vol. 4, p. 2421.
- ⁹See, for example, A. Shastri, F. Borsa, D. R. Torgeson, J. E. Shield, and A. I. Goldman, *Phys. Rev. B* **50**, 15 651 (1994), and references therein.
- ¹⁰A. Viano, Ph.D. thesis, Washington University, St. Louis, MO, 1996.
- ¹¹A. M. Viano, A. F. McDowell, M. S. Conradi, P. C. Gibbons, and K. F. Kelton, in *Proceedings of the Fifth International Conference on Quasicrystals*, edited by C. Janot and R. Mosseri (World Scientific, Singapore, 1995), p. 798.
- ¹²E. Majzoub (unpublished).
- ¹³J. L. Libbert and K. F. Kelton, *Philos. Mag. Lett.* **71**, 153 (1995); *J. Non-Cryst. Solids* **153&154**, 53 (1993).
- ¹⁴E. Majzoub (private communication).
- ¹⁵A. Abragam, *Principles of Nuclear Magnetism* (Clarendon, Oxford, 1961). For discussion of second moments, see pp. 112, 123, and 125; for relaxation rates, see pp. 291 and 457.
- ¹⁶Switendick, *Z. Phys. Chem. (Leipzig)* **117**, 89 (1979).
- ¹⁷W. J. Kim, P. C. Gibbons, and K. F. Kelton, *Philos. Mag. Lett.* (to be published).
- ¹⁸D. G. Westlake, *J. Less-Common Met.* **75**, 177 (1980).
- ¹⁹N. Bloembergen, E. M. Purcell, and R. V. Pound, *Phys. Rev.* **73**, 679 (1948).
- ²⁰J. T. Markert, E. J. Cotts, and R. M. Cotts, *Phys. Rev. B* **37**, 6446 (1988).
- ²¹A. F. McDowell and R. M. Cotts, *Z. Phys. Chem. (Munich)* **183**, 1087 (1994).
- ²²J. W. Han, C.-T. Chang, D. R. Torgeson, E. F. W. Seymour, and R. G. Barnes, *Phys. Rev. B* **36**, 615 (1987); R. L. Lichty, J. W. Han, R. Ibanez-Meier, D. R. Torgeson, R. G. Barnes, E. F. W. Seymour, and C. A. Sholl, *ibid.* **39**, 2012 (1989).
- ²³J. Shinar, D. Davidov, and D. Shaltiel, *Phys. Rev. B* **30**, 6331 (1984).
- ²⁴I. Svare, D. R. Torgeson, and F. Borsa, *Phys. Rev. B* **43**, 7448 (1991).